doi:10.1111/evo.13430

Anatomical network analysis of the musculoskeletal system reveals integration loss and parcellation boost during the fins-to-limbs transition

Borja Esteve-Altava,[1,2,3] Julia L. Molnar,[2] Peter Johnston,[4] John R. Hutchinson,[1] and Rui Diogo[2]

[1]*Structure and Motion Lab, Department of Comparative Biomedical Sciences, Royal Veterinary College, United Kingdom*

[2]*Department of Anatomy, Howard University College of Medicine, Washington, District of Columbia 20059*

[3]*E-mail: bestevealtava@rvc.ac.uk*

[4]*Department of Anatomy and Medical Imaging, University of Auckland, New Zealand*

Received March 21, 2017

Accepted January 14, 2018

Tetrapods evolved from within the lobe-finned fishes around 370 Ma. The evolution of limbs from lobe-fins entailed a major reorganization of the skeletal and muscular anatomy of appendages in early tetrapods. Concurrently, a degree of similarity between pectoral and pelvic appendages also evolved. Here, we compared the anatomy of appendages in extant lobe-finned fishes (*Latimeria* and *Neoceratodus*) and anatomically plesiomorphic amphibians (*Ambystoma*, *Salamandra*) and amniotes (*Sphenodon*) to trace and reconstruct the musculoskeletal changes that took place during the fins-to-limbs transition. We quantified the anatomy of appendages using network analysis. First, we built network models—in which nodes represent bones and muscles, and links represent their anatomical connections—and then we measured network parameters related to their anatomical integration, heterogeneity, and modularity. Our results reveal an evolutionary transition toward less integrated, more modular appendages. We interpret this transition as a diversification of muscle functions in tetrapods compared to lobe-finned fishes. Limbs and lobe-fins show also a greater similarity between their pectoral and pelvic appendages than ray-fins do. These findings on extant species provide a basis for future quantitative and comprehensive reconstructions of the anatomy of limbs in early tetrapod fossils, and a way to better understand the fins-to-limbs transition.

KEY WORDS: **Extant phylogenetic bracketing, pectoral-pelvic similarity, sarcopterygii, serial homology, similarity bottlenecks.**

The limbs of tetrapods evolved from the lobe-fins of sarcopterygian fishes around 370 Ma through a series of anatomical innovations (Fig. 1A). Although at first sight the limbs and lobe-fins of extant species look different, they share some deep similarities in their anatomical organization—the way in which bones and muscles are arranged together—that reveal their common origin. The study of the origin of limbs involves working with uncertain homologies between anatomical structures, reconstructing soft tissue in transitional fossil taxa, and gathering information from the few extant taxa close to the fins-to-limbs transition (e.g., Molnar et al. 2017). These circumstances present a challenge for quantitative methods comparing the anatomical organization of appendages, especially in very disparate forms.

To overcome this problem, here we propose to, and exemplify the use of, a systems biology approach to the study of the fins-to-limbs transition. A systems biology approach to anatomy focuses on the quantification and comparison of anatomical organization, which other properties such as integration, modularity, and functioning depend on (Rasskin-Gutman and Esteve-Altava 2014). The intuitive notion of anatomical organization evokes a group of parts establishing physical interactions that define the overall structure and function of a system (Weiss 1971). Here, we formalized the anatomical organization of fins and limbs using network models that capture the basic physical relationships among bones and muscles. Working with network models of the musculoskeletal anatomy of appendages allows us to directly

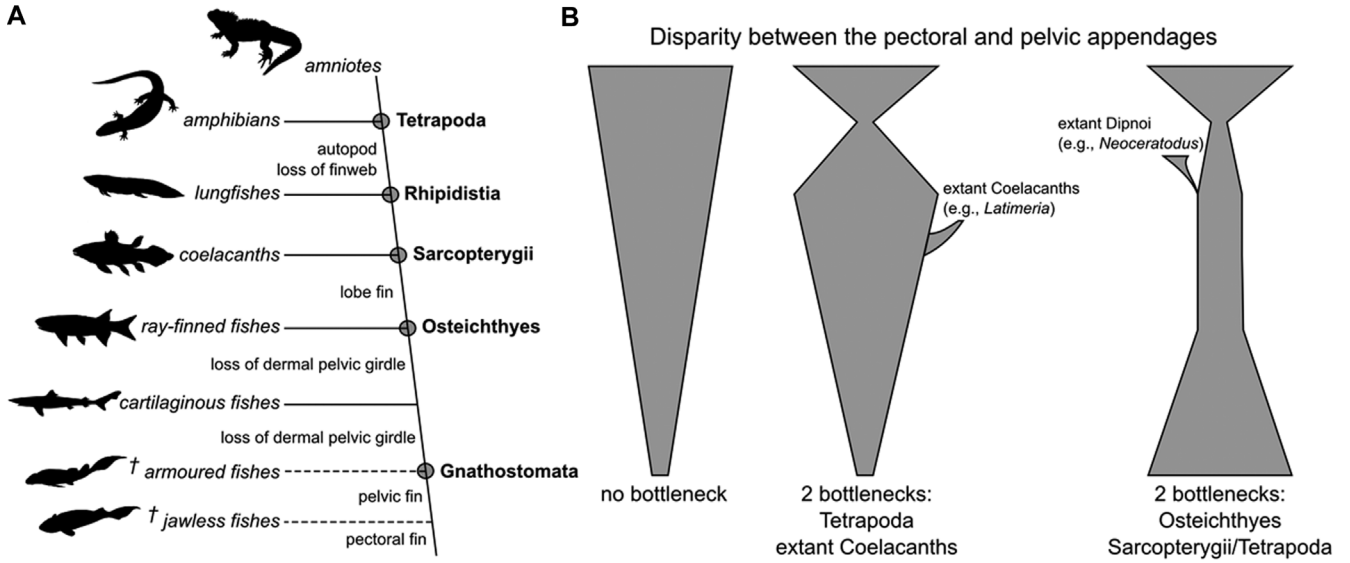

Figure 1. **Diagram of the evolution of limbs from fins. (A) Major evolutionary innovations leading to the origin of modern limbs. (B) Alternative hypotheses proposed to describe the pattern of evolution of the pectoral-pelvic similarity (see *Text* for details). The horizontal length of each funnel indicates figuratively the relative anatomical disparity between pectoral and pelvic appendages for each group in the left cladogram.**

compare forms with incomplete homologies (Diogo et al. 2015), to integrate skeletal and muscular data (Diogo et al. 2015; Molnar et al. 2017; Santos et al. 2017), and to quantify patterns of morphological complexity, integration, and modularity in a manner not available for comparative methods that focus on shape and size (Kerkman et al. 2017; Esteve-Altava 2017a; Murphy et al. 2018).

Anatomical organization has traditionally helped in identifying homologies among disparate taxa (e.g., Remane 1956; Jardine 1969). Homologies are generally more straightforward for the bones and muscles of the girdle, stylopod (arm/thigh), and zeugopod (forearm/leg), because more proximal regions of appendages tend to preserve their anatomical organization across species more often (Diogo and Abdala 2010). One example is the homology between the two most proximal mesomeres and the first radial of lobe-fins and the humerus, radius, and ulna of tetrapod forelimbs, respectively (Coates et al. 2002). Another example is the homology between the adductor profundus muscle of lobe-fins and the puboischiofemoralis internus muscle of limbs (Diogo et al. 2016). In contrast, homologies between more distal regions of appendages are far more controversial, because phylogenetically distant species barely share their anatomical organization in these regions, if at all. For example, there is still debate on whether tetrapod autopod (hand/foot) are homologous to any fin structure or if they evolved de novo (Sordino et al. 1995; Johanson et al. 2007; Woltering and Duboule 2010; Nakamura et al. 2016). Furthermore, the same uncertainty applies to the origin of autopod intrinsic muscles (Diogo et al. 2016). Uncertainties in homologies between lobe-fins and limbs pose a problem to quantitative comparative analyses of their anatomical organization and morphology, limiting such comparisons to a few anatomical elements or to general developmental patterns.

Bones and muscles are equally important in measuring the anatomical organization of appendages and reconstructing the evolution of limbs from lobe-fins. However, most studies on the origin and evolution of limbs focus almost exclusively on the appendicular skeleton. Because skeletons fossilize more easily than soft tissues, they provide direct evidence of the evolution of appendages. For example, from fossils of early Devonian Sarcopterygii we know that tetrapodomorphs already had elbows and knees, and autopods with digits, but that they lacked radials (e.g., Coates and Clack 1990; Coates et al. 2002; Ahlberg 2011). In contrast, we must infer the presence of specific muscles and their attachments in fossil taxa through the scars they left on bones and through phylogenetic inference methods, such as extant phylogenetic bracketing (Witmer 1995). Thus, we rely on the musculoskeletal anatomy of extant species, such as lobe-finned fishes and amphibians (e.g., Boisvert et al. 2013; Diogo et al. 2016; Miyake et al. 2016), to bracket the fins-to-limbs transition and to infer transitional morphologies (Molnar et al. 2017). Likewise, we rely on extant species to understand how the anatomical organization of appendages has evolved, and how pectoral-pelvic similarity changed before and after the fins-to-limbs transition. Furthermore, comparative studies must deal with limitations in the number of specimens available that come from studying scarce fossil materials or rare extant species. These challenges hinder quantitative morphological analysis of important evolutionary events such as the fins-to-limbs transition.

A question that often emerges when studying the origin and evolution of limbs is the apparent similarity in anatomical organization between pectoral and pelvic appendages. Richard Owen labeled pectoral and pelvic appendages as serially homologous, precisely because they shared a similar skeletal anatomy, albeit having different shapes and functions (Owen 1849). Modern evolutionary theory reinterpreted serial homologs as structures derived from evolutionary changes of repeated identical parts in a last common ancestor. The concept of "deep homology," a common developmental-genetic toolkit regulating growth and differentiation of different body parts across distantly related animals (Wagner 1989; Shubin et al. 1997), helped cement the idea that pectoral and pelvic appendages are anatomically similar because pelvic fins evolved by a duplication and redeployment of the same genetic information directing the development of pectoral fins (e.g., Ruvinsky and Gibson-Brown 2000; Young et al. 2005; Abbasi 2011). However, studies in paleontology, comparative muscle anatomy, and development disagree with the conclusion that pectoral and pelvic appendages are serially homologous in a strict modern sense. For example, the fossil record of osteostracans has been interpreted to show that pelvic fins evolved after pectoral fins did, as originally distinct appendages (e.g., pelvic fins lacked a girdle and mineralized radials); and later in evolution pectoral and pelvic fins became more similar (Coates and Cohn 1998, 1999; Diogo et al. 2013; Miyashita and Diogo 2016; but see Wilson et al. 2007 for an alternative explanation due to lack of preservation). It is thought that the first fishes having both pectoral and pelvic fins had, mainly, only adductor and abductor muscle masses, while tetrapods can have up to more than 50 muscles in the anterior and posterior limbs. Because most muscles of the zeugopod and autopod are topologically similar in both limbs, it was inferred that topologically similar muscles evolved independently in the fore- and hindlimbs (i.e., derived topological similarity) (Diogo and Molnar 2014; Diogo and Ziermann 2015; Diogo et al. 2016). Finally, recent studies on genetic regulatory networks have revealed also clear differences in patterns of gene expression between the pectoral and pelvic appendages of tetrapods (Sears et al. 2015). Together, these studies expand a debate on whether pectoral-pelvic similarity evolved by serial homology, by parallelism related to "deep homology," or by convergent evolution.

Linked to the idea of serial homology, the more traditional hypothesis states that pectoral and pelvic appendages originated as mostly identical copies that gradually diversified in form and specialized in function (Fig. 1B left funnel) (reviewed in Diogo et al. 2013). Contrary to this hypothesis, various studies have proposed the presence of derived bottlenecks in pectoral-pelvic similarity within gnathostome evolution. A "similarity bottleneck" is a relatively high degree of similarity between pectoral and pelvic appendages in a particular derived lineage or at an evolutionary event (e.g., during the fins-to-limbs transition). For example, Ahlberg (1989) proposed similarity bottlenecks in the lineage leading to extant coelacanths (*Latimeria*) and at the origin of tetrapods (Fig. 1B central funnel). Others have proposed that pectoral and pelvic fins were originally different and only started to become more similar after a first similarity bottleneck leading to bony fishes and to sarcopterygians, which was followed by a second, more profound similarity bottleneck at the origin of tetrapods (Fig. 1B right funnel) (Coates and Cohn 1998; Coates et al. 2002; Diogo et al. 2013; Diogo and Molnar 2014). These studies have evaluated pectoral-pelvic anatomical similarity mostly by qualitative comparisons of fossils (e.g., Ahlberg 1989; Coates and Cohn 1998; Coates et al. 2002) or by counting topologically equivalent muscles in pectoral and pelvic appendages (Diogo et al. 2013; Diogo and Molnar 2014). Using quantitative tools to measure anatomical organization for entire appendages may help in reconstructing the evolution of the pectoral-pelvic similarity and in testing the presence of such similarity bottlenecks.

Here, we quantified the anatomical organization of extant sarcopterygian appendages (lobe-fins and limbs) to assess how similar they are to each other and how similar their pectoral and pelvic appendages are. Specifically, we tested (1) whether lobe-fins and limbs share a similar underlying anatomical organization or a new organization emerged in tetrapods during the fins-to-limbs transition; (2) whether lobe-finned fishes and tetrapods show equal values of pectoral-pelvic similarity; and (3) whether the evolution of pectoral-pelvic similarity agrees with previously proposed hypotheses on this evolutionary pattern (as described above; Fig. 1B). To answer these questions, we studied the pectoral and pelvic appendages in five extant taxa that phylogenetically bracket the fins-to-limbs transition: two lobe-finned fishes, the African coelacanth *Latimeria chalumnae* and the Australian lungfish *Neoceratodus forsteri*; and three tetrapods, the axolotl *Ambystoma mexicanum*, the fire salamander *Salamandra salamandra*, and the tuatara *Sphenodon punctatus*. As an outgroup for comparison, we also included a representative of the phylogenetically most basal (i.e., widely presumed to have the most plesiomorphic anatomy) extant lineage of ray-finned fishes, the gray bichir *Polypterus senegalus*. See Methods for further details about the selection of taxa.

To quantify the anatomical organization of these appendages, we carried out an anatomical network analysis. First, we built skeletal and muscular network models that capture the gross anatomy of appendages (Fig. 2). A network model comprises nodes that formalize discrete anatomical parts—bones and muscles—and links that formalize pair-wise physical connections among them. Next, we measured a set of seven network parameters to quantify anatomical organization, namely: number of nodes (N), number of links (K), density of connections (D), mean clustering coefficient (C), mean shortest path

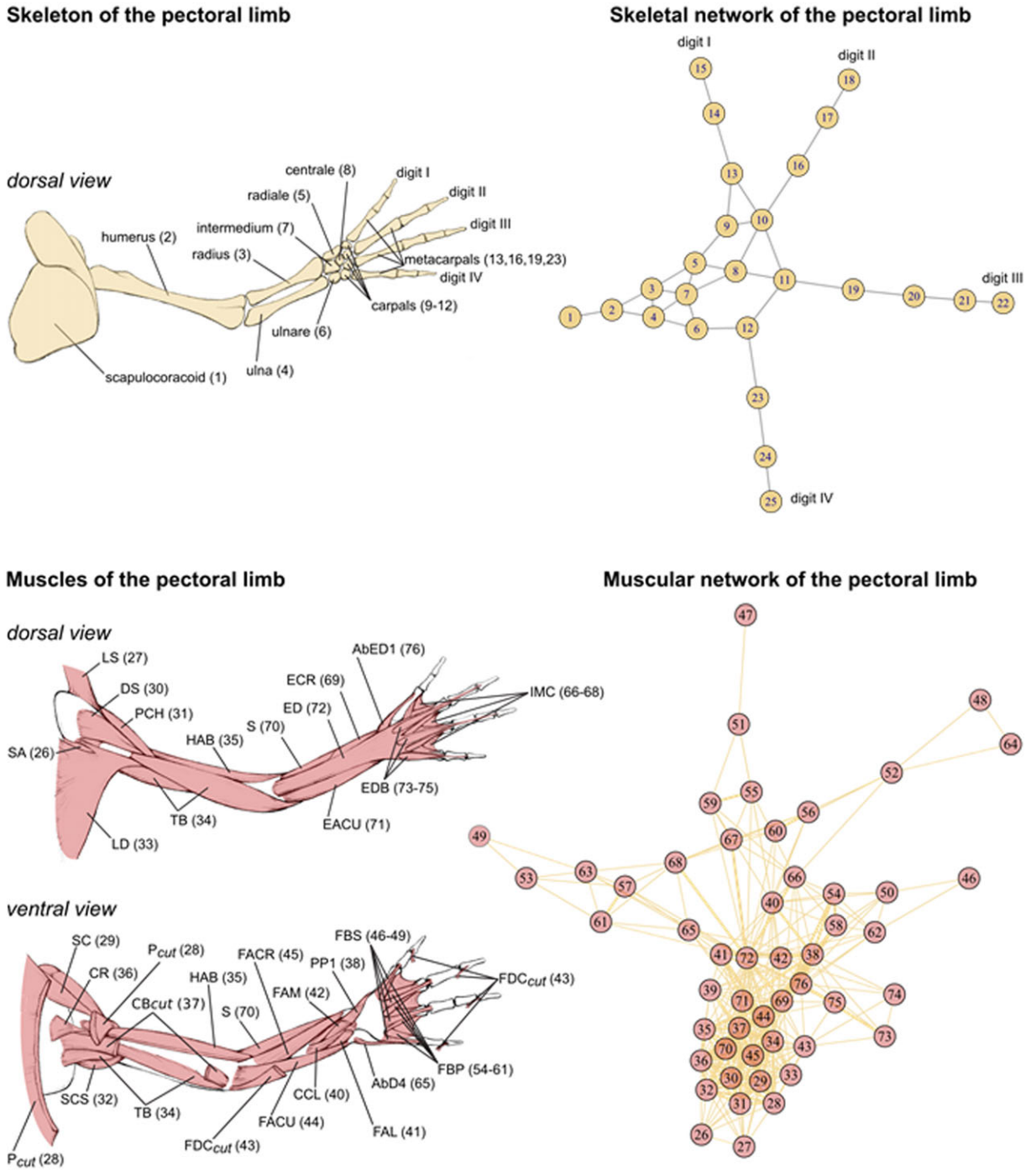

Figure 2. Example of the network modeling approach of a forelimb of a generalized salamander. In the skeletal network (*top*), nodes formalize skeletal elements (bones + cartilages) and links formalize the presence of an articulation between two elements. In the muscular network (*bottom*), nodes formalize muscles and links formalize common anchoring to a same skeletal element. The weight of links in muscular networks captures the number of anchoring skeletal elements in common (the thicker the line, the more anchors in common two muscles have). Pectoral and pelvic appendages of other taxa were modeled likewise. Muscles shown in the anatomical drawings: *SA, serratus anterior; LS, levator scapulae; P, pectoralis; SCR, supracoracoideus; DS, deltoideus scapularis; PCH, procoracohumeralis; SCS, subcoracoscapularis; LD, latissimus dorsi; TB, triceps brachii; HAB, humeroantebrachialis; CR, coracoradialis; CB, coracobrachialis; PP1, palmaris profundus of digit 1; FAL, flexor accessorius lateralis; FAM, flexor accessorius medialis; FDC, flexor digitorum communis; FACU, flexor antebrachii et carpi ulnaris; FACUR, flexor antebrachii et carpi radialis; FBS, flexores breves superficiales, FBP, flexores breves profundus; AbD4, abductor digiti minimi; IMC, intermetacarpales; ECR, extensor carpi radialis; S, supinator; EACU, extensor antebrachii et carpi ulnaris; ED, extensor digitorum; EDB, extensores digitorum breves; AbED1, abductor et extensor of digit 1.*

length (L), heterogeneity of connections (H), and parcellation (P). Figure 3 shows the calculation of these parameters in a toy-example network (see Methods for further details). Network parameters serve as quantitative descriptors of anatomy, but they also carry morphological and functional information. This information derives from the underlying processes of development, which are inherited from one generation to another, and from the role of connections in force transmission among bones and muscles. Box 1 summarizes the morphofunctional interpretation of network parameters as proposed in previous studies (Esteve-Altava et al. 2011; Rasskin-Gutman and Esteve-Altava 2014); we used these interpretations to discuss our results. Finally, we compared the similarity among species' appendages and between pectoral and pelvic appendages, as the relative difference for each parameter and on average.

BOX 1: Morphological interpretation of network parameters

Network nodes (*N*): interacting components of the anatomical structure, for example, bones and muscles.

Network links (*L*): interactions or relations among components, for example, physical contacts. Links may directly or indirectly contribute to biological processes, such as growth or function.

Density of connections (*D*): richness or complexity of the anatomical structure. Also anatomical integration, as it relates to the number of interactions.

Mean clustering coefficient (*C*): anatomical integration, as it relates to functional and/or developmental interdependence among triplets of components.

Mean shortest path length (*L*): anatomical integration, as it relates to the effective proximity between components that allows coordination, independently of their spatial or geometric distance.

Heterogeneity of connections (*H*): differentiation or anisomerism of components in the anatomical structure. Also irregularity, as it contrasts with regular structures (zero heterogeneity).

Parcellation (*P*): degree of modularity of the anatomical structure; how well distributed are the components into the largest number of modules possible.

Results

We measured seven network parameters that capture the anatomical organization of pectoral and pelvic appendages of extant taxa bracketing the fins-to-limbs transition (Table 1 for skeletal networks; Table 2 for muscular networks). We quantified the similarity of anatomical organization among species and between pectoral and pelvic appendages as the pair-wise relative difference (d_r). A lower value of d_r indicates a greater similarity between two appendages. Tables S1–S6 show the exact values of d_r for each comparison in skeletal and muscular networks.

COMPARISON OF SKELETAL NETWORKS

The skeletons of fore- and hind limbs of tetrapods (Fig. 4) have more elements (N) than the pectoral and pelvic ray-fins of *Polypterus* and lobe-fins of *Latimeria*, but fewer than the lobe-fins of *Neoceratodus*. This difference between *Latimeria* and *Neoceratodus* is due to the derived anatomy of *Neoceratodus* fins, which are composed of a long series of mesomeres (up to 14), each one articulating with preaxial and postaxial radials (for a total $N = 55$ and $N = 65$ skeletal elements in the pectoral and pelvic fin, respectively). The number of articulations among skeletal elements (K) follows a similar evolutionary pattern, with *Latimeria* having values within the range of tetrapods. However, the evolution of D, C, and L suggests a partial decrease of anatomical integration in limbs compared to fins and reconstructed ancestral character states: lower D, constant C, greater L. Tetrapods, and *Neoceratodus* have lower values of D in pectoral and pelvic appendages compared to ancestral state reconstructions and to *Latimeria* and *Polypterus*. In turn, the values of C in tetrapods and *Neoceratodus* are more similar to those of ancestral state reconstructions than in the coelacanth *Latimeria*, whereas *Polypterus* has the lowest values for both appendages. Inversely to D, the parameter L increases notably in limbs compared to ancestral state reconstructions, lobe-fins, and ray-fins. At the same time, parameter H in skeletal networks has similarly low values in tetrapods and *Latimeria*, relative to ancestral state reconstructions, *Neoceratodus*, and *Polypterus*. The relatively high H of *Neoceratodus* might be again due to the apomorphic anatomy of *Neoceratodus* fins with a large series of radials (poorly connected, 2–3 connections each) all articulating with the lepidotrichia (highly connected); thus increasing the ratio between variance and mean of connections among elements. The observation that *Latimeria* has a similar H to tetrapods is presumably due to the fact that their lepidotrichia are more distal, and only contact to the most distal radials; whereas in *Neoceratodus* and *Polypterus* the lepidotrichia occupy a broader preaxial and postaxial area and contact all radials. Finally, the evolution of P shows that lobe-fins and limbs have a similarly greater parcellation compared to the ray-fins of *Polypterus* (especially in the pelvic appendage), with *Latimeria* showing the lowest values of all sarcopterygians and *Neoceratodus* showing values close to the reconstructed ancestral state of Tetrapoda (Tables S12–S13). In general, lobe-fins and limbs deviate greatly from the low values of P in *Polypterus* ray-fin skeleton. This pattern is consistent with the aforementioned decrease of integration in the skeletal networks of limbs.

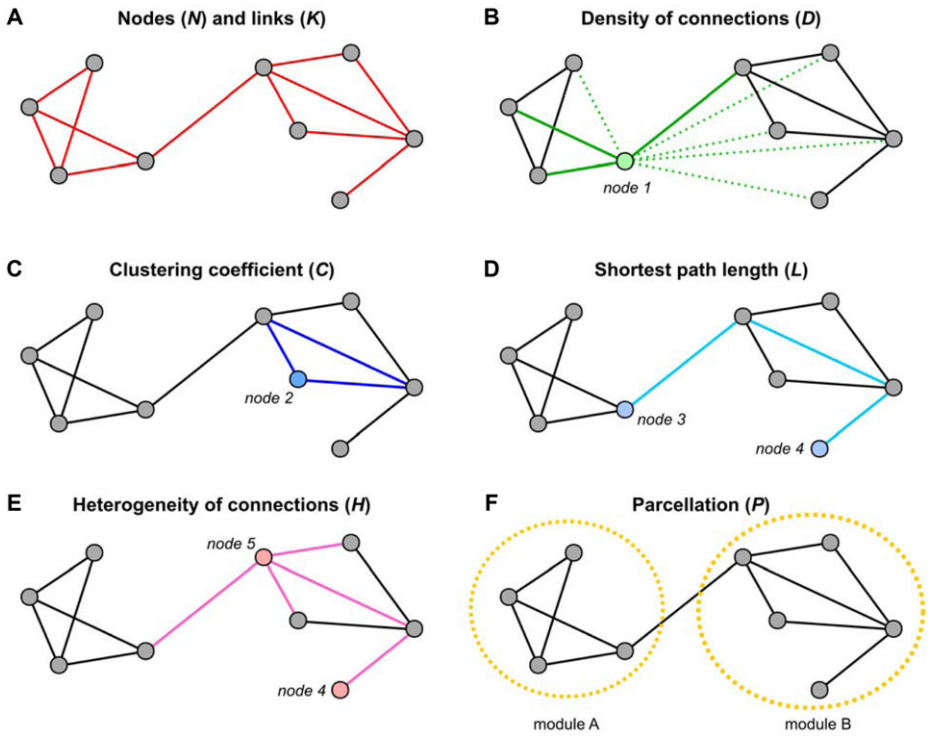

Figure 3. Visual description of the network parameter analyzed. (A) The number of nodes in this network are colored as gray dots ($N = 9$) and the number of links as red lines ($K = 12$). (B) Density (D) is calculated for the entire network; here we show an example with only one node. Node 1 has three realized connections (solid green) and five possible but not realized connections (dashed green); thus, $D_{node1} = 3/8$. (C) Clustering coefficient (C) is calculated for the entire network; here we show an example with only one node. Node 2 (in blue) has only two neighbors, which are in turn connected to each other (solid blue), forming a 3-node loop or triangle. Because all neighbors of node 2 are connected among them, $C_{node2} = 1$. (D) Shortest path length (L) is calculated for the entire network; here we show an example with only two nodes. Three links (in cyan) are the minimum number of links required to connect node 3 and node 4; thus, $L_{node3,\ node4} = 3$. (E) Heterogeneity (H) is calculated for the entire network; here we show an example with only two nodes. Nodes 4 and 5 have a different number of connections, one and four, respectively. If we only consider these two nodes, then $H \approx 2.1/2.5 = 0.84$. (F) Parcellation (P) is calculated after a community detection algorithm has identified the connectivity modules; two in this example: module A and module B (dashed yellow circles). Module A has four nodes and module B has five nodes of a total of nine nodes in the network; thus, $P = 1 - [(4/9)^2 + (5/9)^2] = 0.49$. If the network were divided less uniformly, for example, into one large module of seven nodes and one small module of two nodes, then $P = 1 - [(7/9)^2 + (2/9)^2] = 0.35$. In contrast, if the nine nodes of the network were divided into three modules of equal size (i.e., three 3-node modules), then $P = 1 - [(3/9)^2 + (3/9)^2 + (3/9)^2] = 0.67$.

Table 1. Network parameters measured in skeletal networks.

Skeletal network	N	K	D	C	L	H	P
Polypterus pectoral appendage	47	84	0.078	0.086	2.988	0.937	0.830
Polypterus pelvic appendage	9	9	0.250	0	2.167	0.612	0.642
Latimeria pectoral appendage	24	44	0.159	0.503	3.478	0.525	0.715
Latimeria pelvic appendage	22	42	0.182	0.353	2.593	0.482	0.740
Neoceratodus pectoral appendage	55	102	0.069	0.127	2.782	1.304	0.818
Neoceratodus pelvic appendage	64	133	0.066	0.142	2.327	1.468	0.794
Ambystoma pectoral appendage	25	35	0.117	0.227	3.870	0.515	0.778
Ambystoma pelvic appendage	32	44	0.089	0.244	4.518	0.522	0.820
Salamandra pectoral appendage	25	34	0.113	0.197	4.000	0.526	0.816
Salamandra pelvic appendage	32	42	0.085	0.201	4.669	0.491	0.820
Sphenodon pectoral appendage	37	47	0.071	0.159	5.240	0.496	0.844
Sphenodon pelvic appendage	31	36	0.077	0.151	4.910	0.514	0.849

Table 2. Network parameters measured in muscular networks.

Muscular network	*N*	*K*	*D*	*C*	*L*	*H*	*P*
Polypterus pectoral appendage	6	15	1	1	1	0	0.500
Polypterus pelvic appendage	3	3	1	1	1	0	0
Latimeria pectoral appendage	19	112	0.655	0.781	1.363	0.263	0.571
Latimeria pelvic appendage	15	82	0.781	0.915	1.219	0.278	0.498
Neoceratodus pectoral appendage	5	7	0.700	0.875	1.300	0.391	0.480
Neoceratodus pelvic appendage	37	461	0.692	0.955	1.308	0.323	0.777
Ambystoma pectoral appendage	51	309	0.242	0.733	2.136	0.633	0.700
Ambystoma pelvic appendage	59	294	0.172	0.700	2.130	0.578	0.783
Salamandra pectoral appendage	50	292	0.238	0.724	2.153	0.621	0.631
Salamandra pelvic appendage	59	290	0.169	0.703	2.181	0.571	0.784
Sphenodon pectoral appendage	49	415	0.353	0.805	1.771	0.598	0.591
Sphenodon pelvic appendage	50	364	0.297	0.712	1.827	0.328	0.630

Regarding the similarity of the pectoral skeleton among the taxa analyzed (Table S1), on average the greatest disparity occurs between the pectoral lobe-fins of *Latimeria* and *Neoceratodus* (d_r = 68%), whereas the lowest disparity occurs, as expected, between *Salamandra* and *Ambystoma* (d_r = 4%). The disparity between the pectoral ray-fins of *Polypterus* and pectoral lobe-fins and limbs is almost as wide (d_r = 18–61%) as it is between pectoral lobe-fins and limbs (d_r = 22–58%). Also, the disparity between the pectoral lobe-fins of *Latimeria* and of *Neoceratodus* is greater (d_r = 68%) than it is among the pectoral limbs of *Ambystoma*, *Salamandra*, and *Sphenodon* (d_r = 4–28%). Without muscles, the pectoral limbs of tetrapods are more similar (i.e., less disparity) to the pectoral lobe-fins of *Latimeria* (d_r = 22–42%) than to that of *Neoceratodus* (d_r = 42–58%). Interestingly, over the average of all comparisons, parameter *P* shows the lowest disparity (d_r = 7%) compared to all other parameters (d_r = 27–66%), which makes the degree of modularity the least variable feature of the anatomical organization among the pectoral appendages studied. In turn, in the pelvic skeleton (Table S2) the greatest disparity occurs between the pelvic ray-fins of *Polypterus* and the pelvic lobe-fins of *Neoceratodus* (107%), whereas the lowest disparity occurs, again, between *Salamandra* and *Ambystoma* (d_r = 5%). The disparity between the pelvic ray-fins of *Polypterus* and pelvic lobe-fins and limbs is greater (d_r = 72–107%) than it is between pelvic lobe-fins and limbs (d_r = 31–59%). Furthermore, the disparity between the pelvic lobe-fins of *Latimeria* and of *Neoceratodus* is greater (d_r = 71%) than it is among the pelvic limbs of *Ambystoma*, *Salamandra*, and *Sphenodon* (d_r = 5–14%). Without muscles, the pelvic limbs of tetrapods are more similar to the pelvic lobe-fins of *Latimeria* (d_r = 31–42%) than to the lobe-fins of *Neoceratodus* (d_r = 54–59%). Again, *P* shows the lowest disparity (d_r = 12%) of all other parameters (d_r = 39–96%), which makes the degree of modularity the least variable organizational feature also among pelvic appendages.

COMPARISON OF MUSCULAR NETWORKS

The muscular system of fore- and hind limbs of tetrapods (Fig. 5) has more muscles (*N*) than in lobe-fins, ray-fins, and ancestral state reconstructions. The lobe-fins of *Latimeria* and *Neoceratodus* also have more muscles than the ray-fins of *Polypterus*. The number of connections among muscles (*K*, i.e., common anchoring sites) follows the same evolutionary pattern. However, in both parameters, the pectoral fin musculature of *Neoceratodus* is more similar to that of *Polypterus* than that of *Latimeria* and tetrapods. This is because, as in *Polypterus*, the pectoral fins of *Neoceratodus* have only a few differentiated muscles: retractor lateralis ventralis pectoralis, superficial abductor, and adductors, and deep abductor and adductor. As in the skeletal network evolution, the patterns inferred for *D*, *C*, and *L* portray a marked trend toward a decrease in anatomical integration of the muscular system from fins to limbs. The network of muscles in tetrapod limbs has lower *D* and *C* and higher *L* than the ancestral state reconstructions for lobe-fins and ray-fins. The decrease in anatomical integration is notable in salamanders compared to *Sphenodon*, with the limbs of the tuatara showing values closer to those for ancestral state reconstructions of tetrapods. In line with this trend, the lobe-fins of *Latimeria* and *Neoceratodus* have higher *D* and *C*, and lower *L*, than ancestral state reconstructions. The pectoral and pelvic ray-fins of *Polypterus* show extreme values of D, C, L, and H, because of the presence of only a few muscles sharing common sites of attachments (6 and 3, respectively) completely interconnected to each other. The evolution of *H* in muscular networks points to the presence of a shift toward greater differentiation/specialization of muscles in limbs (higher *H*) compared to ancestral state reconstructions and to lobe-fins. This shift is more pronounced in the pectoral appendages and less pronounced in the pelvic appendages. Similar to the results for integration parameters, the limbs of *Sphenodon* present values that are closer to those of ancestral state reconstructions of tetrapods. Lastly, the

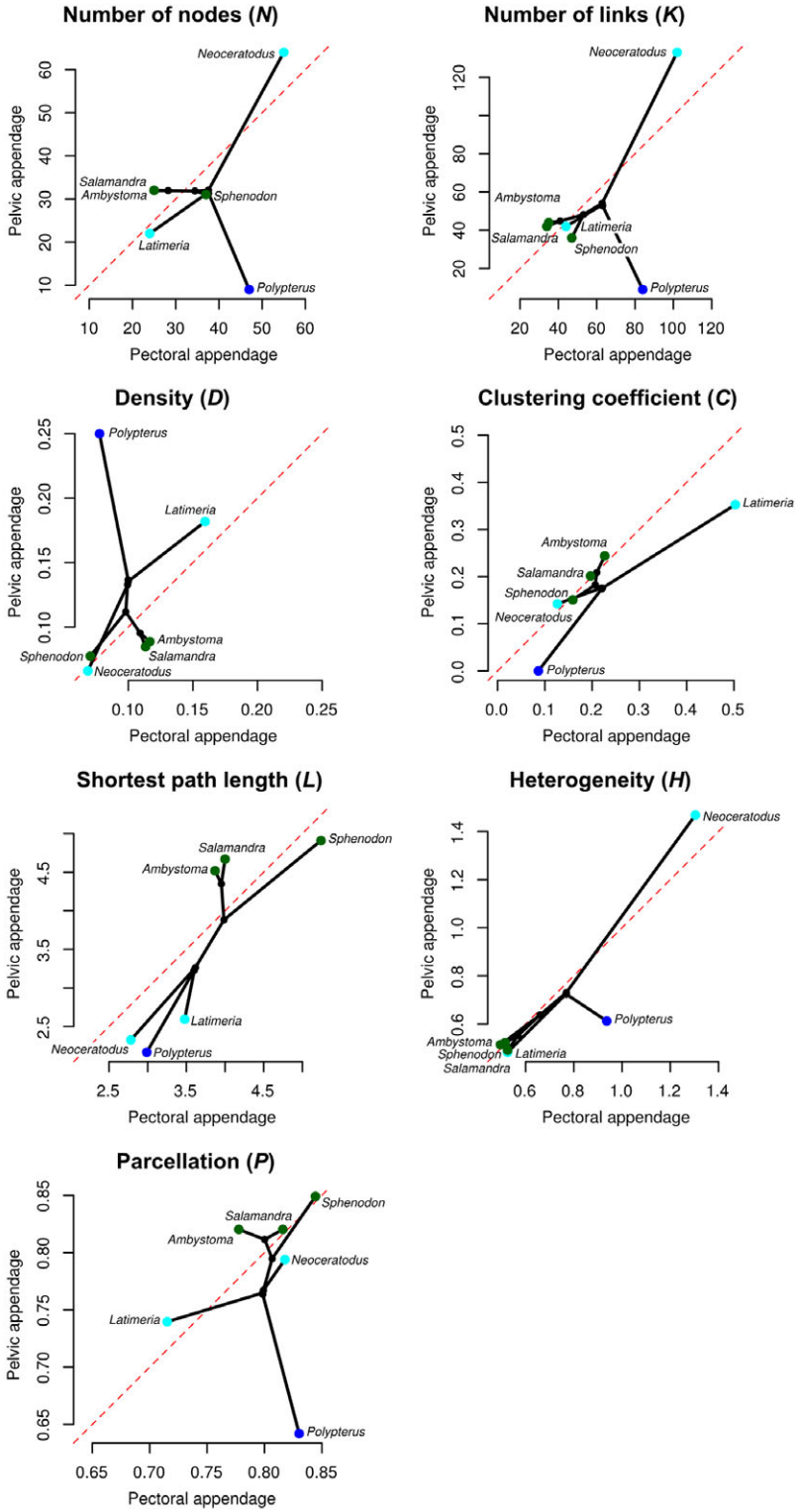

Figure 4. Phylomorphospaces of the skeletal networks of analyzed taxa. Parameters compared include number of skeletal elements (*N*), number of articulations or joints (*K*), density of connections (*D*), average clustering coefficient (*C*), average shortest path length (*L*), heterogeneity of connections (*H*), and parcellation (*P*). Parameter values of pectoral and pelvic appendages are represented in the horizontal and vertical axis, respectively, for each taxon. Tip colors indicate the type of appendage: ray-fin (dark blue), lobe-fin (cyan), and limb (green). The dashed red line marks the identity line or maximum pectoral-pelvic similarity. The values for the hypothetical ancestral states within the phylogeny (black dots) were estimated by maximum likelihood on a time-calibrated phylogeny (see Methods for details).

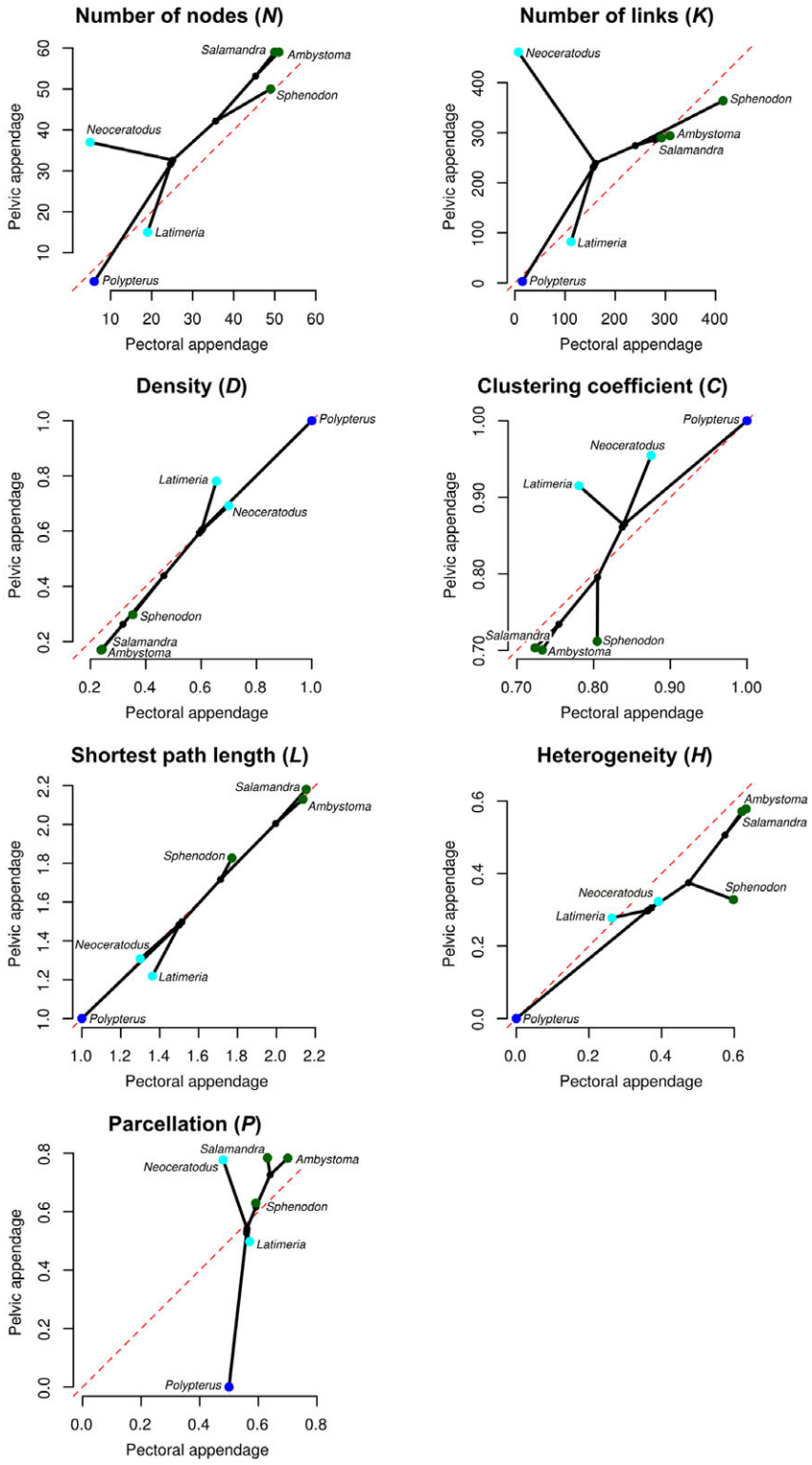

Figure 5. Phylomorphospaces of the muscular networks of analyzed taxa. Parameters compared include number of skeletal elements (*N*), number of articulations or joints (*K*), density of connections (*D*), average clustering coefficient (*C*), average shortest path length (*L*), heterogeneity of connections (*H*), and parcellation (*P*). Parameter values of pectoral and pelvic appendages are represented in the horizontal and vertical axis, respectively, for each taxon. Tip colors indicate the type of appendage: ray-fin (dark blue), lobe-fin (cyan), and limb (green). The dashed red line marks the identity line or maximum pectoral-pelvic similarity. The values of the hypothetical ancestral states within the phylogeny were estimated by maximum likelihood on the time-calibrated phylogeny (see Methods for details).

evolution of *P* shows also a shift toward a greater parcellation of the appendages, in which limbs are more parcellated than in ancestral state reconstructions, lobe-fins (except for the pelvic fin of *Neoceratodus* that is in the range of the values of *P* in tetrapods), and ray-fins. This pattern is consistent with the aforementioned decrease of integration and increase of differentiation in muscular networks in tetrapods.

Regarding the similarity of the pectoral musculature among the taxa examined (Table S4), on average the greatest disparity occurs between the pectoral ray-fins of *Polypterus* and the pectoral limbs of tetrapods (d_r = 105–114%), while the lowest disparity separates the pectoral limbs of *Ambystoma* and *Salamandra* (d_r = 3%). The disparity between the pectoral ray-fins of *Polypterus* and the pectoral lobe-fins of *Latimeria* and *Neoceratodus* is in the same range (d_r = 53–81%) as it is between pectoral lobe-fins and limbs (d_r = 53–86%); while the disparity between *Latimeria* and *Neoceratodus* pectoral lobe-fins themselves is at the lower side of this range (d_r = 53%). As for the average of parameters, in contrast to the pectoral skeleton, *C* shows the lowest disparities (d_r = 14%) and *P* the second lowest (d_r = 17%) of all other parameters (d_r = 36–126%), which makes the integration by interdependence the least variable organizational feature also among the musculature of pelvic appendages. In pelvic appendages (Table S5), the greatest disparity occurs between the pelvic ray-fins of *Polypterus* and the pelvic limbs of salamanders (d_r = 146–147%), while the lowest disparity occurs, as expected, between the pelvic limbs of *Ambystoma* and *Salamandra* (d_r = 1%). The disparity between the pelvic ray-fins of *Polypterus* and pelvic lobe-fins and limbs is greater (d_r = 110–147%) than it is between pelvic lobe-fins and limbs (d_r = 31–79%). As expected, the lowest disparity occurs among tetrapods limbs (d_r = 1–27%). Likewise in the pelvic musculature, parameter *C* shows the lowest disparities (d_r = 29%) of all other parameters (d_r = 38–108%), which makes the integration by interdependence the least variable organizational of the pelvic musculature.

COMPARISON OF PECTORAL-PELVIC SIMILARITY

Phylomorphospace plots (Figs. 4 and 5) were used to show the evolution of the pectoral-pelvic similarity of appendages; a *red dashed line* marks the equality line (1:1 line) between pectoral and pectoral values. On average, *Polypterus* shows the lowest pectoral-pelvic similarity (i.e., highest percentage of relative difference, d_r) of all studied taxa, both in skeletal networks (d_r = 100%; Tables S3; Fig. S1) and in muscular networks (d_r = 67%; Table S6; Fig. S2). In skeletal networks, the pectoral-pelvic similarity of lobe-fins (*Latimeria*: d_r = 15%; *Neoceratodus*: d_r = 13%) is comparable to that of the limbs of salamanders (d_r = 14–15%), whereas S*phenodon* shows the greatest pectoral-pelvic similarity of all taxa analyzed (d_r = 10%). Among parameters, *P* shows the highest similarity between pectoral and pelvic skeletons (d_r = 6%) of all other parameters (d_r = 12–44%), which indicates that pectoral and pelvic skeletons are not very different in the modular organization of the skeletal anatomy. In muscular networks, the pectoral-pelvic similarity is equally high in *Latimeria*'s lobe-fins (d_r = 17%) and tetrapod limbs (d_r = 11–16%); but it is much lower (d_r = 60%) in *Neoceratodus*. However, this high disparity of *Neoceratodus* at the muscular level is mainly driven by the differences in the number of muscles (five in the pectoral fins and 37 in the pelvic fins) and of contacts (seven and 471, respectively), which is most likely related to a derived reduction of the pectoral fins in Dipnoi. Interestingly, parameters *D*, *C*, *L*, and *H* (which correct for network size) in *Neoceratodus* show relative differences in muscular networks that are closer to those of *Latimeria* and tetrapods; excluding *N* and *K*, pectoral-pelvic relative difference in *Neoceratodus* muscular networks average only 15%. Among parameters, *L* and *C* show the highest similarity between pectoral and pelvic musculatures ($L\ d_r$ = 3%; $C\ d_r$ = 7%) of all other parameters (d_r = 20–73%), which indicates that pectoral and pelvic musculature established similar degrees of anatomical integration of connections. Both skeletal and muscular evolutionary patterns of the pectoral-pelvic similarity reported are in line with the presence of a similarity bottleneck in the hypothetical ancestor of sarcopterygians, but not a second similarity bottleneck at the origin of tetrapods. The secondary increase of disparity in *Neoceratodus* (as expected in the hypothesis illustrated in the right funnel of Fig. 1B, and most likely related to a secondary reduction of pectoral fins in Dipnoi) is only observed at the muscular level for the number of muscles (*N*) and their connections (*K*). In contrast, parameters measured in muscular networks related to anatomical integration (*D*, *C*, *L*), differentiation (*H*), and modularity (*P*) show that *Neoceratodus* pectoral-pelvic similarity is in the range values observed for *Latimeria* and tetrapods. Finally, the ancestral state reconstructions of sarcopterygians and tetrapods tend to occupy positions in the phylomorphospaces of skeletal and muscular networks that are closer to the maximum pectoral-pelvic similarity (Figs. 4 and 5). However, a broader sample of taxa would be needed to conclusively map the positions of hypothetical last common ancestors in these morphospaces.

Discussion

DISINTEGRATION, SPECIALIZATION, AND PARCELLATION OF LIMBS

Our results show that the anatomical integration of the appendages (as estimated by proxies *D*, *C*, and *L*) decreased from lobe-fins to limbs. This is an evolutionary pattern we see in both the pectoral and pelvic appendages. This pattern is consistent with a transition from a web-like appendage of interconnecting bones, as in coelacanths and extinct tetrapodomorphs (e.g., *Tiktaalik*; Shubin et al.

2006, 2014), to a more tree-like appendage with digits and series of phalanges in tetrapods. In this context, the tree-like organization of *Neoceratodus* would be a secondarily derived feature or convergence, which comes from the radial structure of the fins, rather than the presence of digits with phalanges. Because tetrapods still conserve part of a web-like arrangement among the mesopod bones, their values of clustering (*C*) did not decrease compared to *Neoceratodus* lobe-fins and *Polypterus* ray-fins, which lack such an arrangement in any part of their fins. Moreover, most newly evolved muscles have fewer attachments (i.e., connections) compared to the undivided muscle masses of lobe-fins (e.g., deep and superficial adductors and abductors) (Diogo et al. 2016). Together, these findings suggest that the increased number of autopodial bones and newly differentiated muscles in evolving limbs was not accompanied by a proportional increase of new physical contacts. Hence, limbs became less anatomically integrated compared to lobe-fins.

Another consequence of limbs being sparsely integrated compared to fins is the increase of modularity or parcellation in limbs, both at a skeletal and a muscular level. In morphology, integration and modularity are largely opposite properties, with modules originating because of a loss of integration at the boundary of two or more regions (Simon 1962; Eble 2005; Wagner et al. 2007; Klingenberg 2008; Goswami et al. 2015; Esteve-Altava 2017a, 2017b). The proxy used to evaluate the parcellation of fins and limbs in anatomical networks (*P*) shows a marked shift toward an increase of modularity from fins to limbs. This means that tetrapod limbs have more, and more balanced, modules than ray-fins. In this scenario of increasing modularity, lobe-fins adopted intermediate values between ray-fins and limbs, as expected by their phylogenetic position. This may indicate that evolving a greater degree of modularity of appendages was a novelty acquired prior to the fins-to-limbs transition, which was later reinforced in tetrapods.

Here, we show also that integration and parcellation have evolved differently for the skeletal and for the muscular components of appendages. Anatomical parcellation is the most similar organizational feature among skeletons of different taxa and between pectoral and pelvic appendages of the same taxon. In contrast, anatomical integration (specifically, *C* and *L*) is the most similar feature for the musculature, for all comparisons among and within appendages. Although coordinated morphological responses are necessary for organisms to adapt to new conditions, bones and muscles respond differentially in time and magnitude to evolutionary pressures (Diogo et al. 2013). This difference between skeletal and muscular networks suggests a decoupled modularity response to different functional demands for the skeleton and the musculature during evolution. Further studies including more taxa, and in different groups, will be needed to test this preliminary inference.

In tandem with the relative reduction in anatomical integration in tetrapods, muscle groups also changed their connectivity patterns, becoming more functionally specialized in tetrapods than in lobe-finned fishes (Diogo et al. 2016). The evolution of heterogeneity (*H*) or anisomerism in muscular networks matches this specialization of appendicular muscles. In fins, muscle masses are few and similarly connected (lower *H*), and tend to be more generalized in their potential actions (e.g., adductor and abductor muscles) (Diogo et al. 2016; Molnar et al. 2016, 2017). In limbs, we find a wider variety of muscles between two extremes (higher *H*): some limb muscles establish a few short-range connections and function more locally (e.g., intermetatarsales, flexores breves profundi, and contrahentes pedis, each of which has two connections), while others establish many long-range connections and function more globally (e.g., flexor digitorum communis, contrahentium caput longum, extensor digitorum longus) (Diogo and Abdala 2010). We speculate that this increase in heterogeneity and specialization of the anatomy of limbs enhanced or facilitated the evolution of a wide range of locomotion strategies within tetrapods.

To what extent is the reported evolution of network integration and parcellation related to variational (shape) and developmental modularity in fins and limbs? This remains highly uncertain. Unfortunately, studies on the morphological integration and modularity of pectoral and pelvic fins are scarce (reviewed in Esteve-Altava 2017b). For example, the modularity of fins has been studied in fishes, comparing patterns of presence and disparity among pectoral, pelvic, dorsal, anal, and caudal fins (Larouche et al. 2015, 2017); however, these studies did not test whether each fin has variational modules or it is entirely integrated. To our knowledge, there are no studies of variational modularity in lobe-fins. The vast majority of studies of morphological integration and modularity in appendages focus on limbs and use morphometrics to assess skeletal shape variation (Esteve-Altava 2017a). These studies found variational modules in many tetrapod groups, including salamanders (Kolarov et al. 2011). However, morphological integration among modules may vary within limbs due to, for example, ecological specialization (Young et al. 2010; Martín-Serra et al. 2015) or developmental stage (Kolarov et al. 2011; Maxwell and Dececchi 2012). On the other hand, developmental studies highlight the differences in modularity we observed in the parcellation of fins and limbs. For example, ray-fins have been suggested to have fewer skeletal compartments or modules (one radial domain + fin ray) than sarcopterygian fins (three endoskeletal domains + fin ray) and limbs (stylopod, zeugopod, and autopod) (Yano and Tamura 2013). In addition, tetrapods have pectoral and pelvic girdles that also show a developmental semi-independence (Sears et al. 2015). From a developmental point of view, some studies have speculated that the different degree of parcellation between fins and limbs might be a consequence of a

combination of various developmental mechanisms; for example, decoupling of the Meis/HoxA11/HoxA13 expression, the more distal and late expansion of the 5'HoxD genes, and timing of the apical ectodermal ridge (AER) to apical fold (AF) transition (Yano and Tamura 2013).

NEOCERATODUS IS AN UNUSUAL FISH

As our results show, the corresponding forelimbs and hindlimbs of the three tetrapod taxa resemble each other more than pectoral and pelvic fins of lobe-finned fishes do, respectively. Interestingly though, lobe-fins vary in their similarity to limbs, with *Latimeria* often being more similar to tetrapods than *Neoceratodus* despite their phylogenetic positions. In fact, most analyses place *Neoceratodus* closer than *Latimeria* to the tetrapod stem (e.g., see Irisarri et al. 2017). *Neoceratodus* deviates from *Latimeria*, for example, in the number of parts, anatomical integration, and parcellation. A closer look at the gross anatomy of *Neoceratodus*, compared to that of *Latimeria*, demonstrates that the lobe-fins of *Neoceratodus* have an extremely derived anatomy, which comprises a long series of mesomeres (often 14, but sometimes more), each accompanied by four or five pre- and postaxial radials. In addition, the musculature of the pectoral fin is secondarily simplified, with only five muscle masses, whereas the pelvic fin presents a sequence of pronator and supinator muscles (one of each for each mesomere) (Diogo et al. 2016). This reduction in number of muscles is most likely related to the secondary (derived) reduction of the pectoral fins of *Neoceratodus* that occurred during dipnoan evolutionary history (Diogo et al. 2016). The anatomy of *Neoceratodus* fins is unusual, especially, when compared with what is known of stem tetrapodomorphs such as *Eusthenopteron* (Andrews and Westoll 1970), *Panderichthys* (Boisvert 2005; Boisvert et al. 2008), or *Tiktaalik* (Shubin et al. 2006, 2014). Only when we compare *Neoceratodus* to extinct porolepiform lobe-finned fishes like *Glyptolepis* (Ahlberg 1989) can we see a similarly derived anatomy, with a long series of mesomeres and radials. Based on our findings about the network topology of lobe-fins and limbs, we infer that *Latimeria* retains more ancestral traits for Sarcoptergii for extant phylogenetic bracketing in reconstructing the muscular anatomy of intermediate forms between lobe-finned sarcopterygians and tetrapods (e.g., Molnar et al. 2017), and for comparisons based on anatomical network analysis. Furthermore, the addition of dipnoan fossils to future analyses could clarify the patterns of change in that clade and more broadly in Sarcopterygii that led to the unusual form of lobe-fins in derived dipnoan taxa such as *Neoceratodus*.

BOTTLENECKS IN PECTORAL-PELVIC SIMILARITY

Ray-fins and sarcopterygian appendages (lobe-fins and limbs) differ in their pectoral-pelvic similarity, whereas lobe-finned fishes and tetrapods have closer values of pectoral-pelvic similarity. Although pectoral-pelvic similarity in lobe-fins is within the range observed in tetrapods for the skeleton, when muscles are compared, *Neoceratodus* deviates from the tetrapod range and occupies an intermediate position between *Polypterus* and tetrapods. However, this deviation is mostly driven by differences in the number of muscles and attachments derived likely from the loss of pectoral fin muscles in *Neoceratodus*, due to a secondary simplification of its pectoral appendages (Diogo et al. 2016). In fact, network parameters related to anatomical integration and heterogeneity indicate that *Neoceratodus* has a pectoral-pelvic similarity partially within the range of tetrapods and *Latimeria* for muscular networks.

On a separate note, studies comparing shape variation between pectoral and pelvic appendages have also reported similarities of morphological integration in tetrapods (Hallgrímsson et al. 2002; Young et al. 2005, 2010; Goswami et al. 2014). These studies often link the presence of similar patterns of morphological integration between fore- and hindlimbs to serial homology and/or to shared developmental toolkits (Wagner 1989, 2014; Shubin et al. 1997; Hallgrímsson et al. 2002). However, patterns of integration of shape covariation between fore- and hindlimbs can change by differential functional specializations of each pair of appendages (Young et al. 2010; Villmoare et al. 2011). Our results at the anatomical network level support the idea of pectoral-pelvic integration in sarcopterygians, which evolved similarly higher anatomical integration compared to nonsarcopterygian fishes with ray-fins.

Finally, our results confirm the presence of a similarity bottleneck leading to sarcopterygians, which is only predicted by one of the three hypotheses presented (Fig. 1B, right funnel). These results partially supports the two-bottleneck hypothesis (osteichthyes and sarcopterygians) proposed by Coates and Cohn (1998), Coates et al. (2002), Diogo et al. (2013), and Diogo and Molnar (2014). However, this hypothesis also predicts an additional bottleneck leading specifically to tetrapods, which we cannot confirm or reject with the anatomical network analysis of appendages. This additional bottleneck is supported by the comparison of the number of muscles and bones that are topologically similar in the pectoral and pelvic appendages (see Diogo et al. 2013; Diogo and Molnar 2014). In general, our findings are in line with the idea that pectoral-pelvic similarity of limbs is mainly due to parallel or convergent evolution within gnathostomes, rather than due to serial homology, because tetrapods show larger average similarities in the organization of the skeleton and muscles of appendages than lobe-finned and ray-finned fish. Future anatomical network studies, including sarcopterygian fish fossils as well as early tetrapod fossils, could further test these ideas and can also help to clarify why some of the network patterns that we found differ between skeletal and muscular structures. We

expect that the findings presented in this study on the anatomical similarities between lobe-fins and limbs, and between pectoral and pelvic appendages, will inform future reconstructions of the musculoskeletal anatomy in such fossil taxa and thus be helpful in gaining a better understanding of the origin and later diversification of tetrapod limbs.

Methods

GATHERING ANATOMICAL INFORMATION

We dissected the pectoral and pelvic appendages of *Polypterus senegalus* (Actinopterygii: Polypteridae), *Latimeria chalumnae* (Sarcopterigii: Coelacanthiformes), *Neoceratodus forsteri* (Sarcopterygii: Dipnoi), *Ambystoma mexicanum* (Urodela: Ambystomatidae), *Salamandra salamandra* (Urodela: Salamandridae), and *Sphenodon punctatus* (Lepidosauria: Rhynchocephalia). All specimens examined were wild-type adults, donated frozen or preserved; no experiments on live animals were performed for this study. Three frozen specimens of *Polypterus senegalus* (HU PS1, HU PS2, and HU PS5-1) were donated by the Department of Anatomy at Howard University College of Medicine, USA, and dissected under magnification. One formalin-fixed specimen of *Latimeria chalumnae* (SZ10378) was dissected and serial histological sections of one embryo of *Latimeria* (CCC163K) were examined at the Institüt für Evolution und Ökologie, Universität Tübingen, Germany. Two formalin fixed specimens of *Neoceratodus forsteri* (JVM-I-1051NC, JVM-I-1052NC) were donated by Macquarie University, Australia, and dissected under magnification. In addition, MRI scans of *Latimeria chalumnae* and *Neoceratodus forsteri* were provided by the Digital Fish Library, UCSD (www.digitalfishlibrary.org). Images were resized in ImageJ (NIH) and 3D reconstruction of fin skeleton and muscles was performed with Amira 5.2.1 (Visage Imaging) with manual segmentation of structures. Three specimens of *Ambystoma mexicanum* (HU AM1, HU AM2, and HU AM5-1) were donated by the Department of Anatomy at Howard University College of Medicine, USA, and dissected under magnification. Five specimens of fire salamanders (*Salamandra salamandra*; Royal Veterinary College (UK) specimens RVC-JRH-SAL1 through SAL5) that had died in captivity from reasons unrelated to this study were dissected under magnification. Two specimens of the tuatara *Sphenodon punctatus* were dissected under magnification; these were "no data" museum specimens (Natural History Museum (London, UK) specimen BMNH1935.12.6.1; California Academy of Sciences (San Francisco, USA) specimen CAS 208882) collected long before our study under unknown conditions. For simplicity, sesamoid bones (e.g., Regnault et al. 2017) were not coded in these networks, nor were soft tissue contacts/attachments such as cartilages and ligaments, but future analyses could add such data.

Taxa were selected because they possess the relatively most plesiomorphic anatomy of appendages of extant taxa bracketing the fins-to-limbs transition (i.e., rootward and crownward relative to Tetrapoda/Amniota) and because they were available for dissection. Thus, we chose tetrapod taxa with plesiomorphic anatomies, such as salamanders and tuatara, and excluded frogs which have highly specialized limbs. Of the two species of extant coelacanth species, *Latimeria chalumnae* (listed as critically endangered by the IUCN) and *Latimeria menadoensis* (listed as vulnerable by the IUCN), only the former was available for dissection and there is no indication that the latter taxon's anatomy is divergent from the former's. Of the six extant species of lungfishes, *Neoceratodus forsteri* is the only one not having extremely simplified appendages. Given the few available taxa of lobe-finned fishes, a larger sample size would only be possible by including more tetrapods (e.g., mammals, crocodiles, turtles). Importantly, we decided not to do this to avoid a bias toward tetrapod forms in our comparisons. Furthermore, it was qualitatively clear to us that the bones and muscles of these amniote taxa are not so divergent that they would greatly alter our conclusions about bottlenecks or general evolutionary patterns (e.g., close to the origin of Tetrapoda or more rootward of it). To minimize potential intraspecific variability in the arrangement of bones and muscles in the taxa selected, we carried out an extensive literature survey (Goodrich 1930; Francis 1934; Millot and Anthony 1958; Young et al. 1989; Diogo and Abdala 2010; Diogo and Tanaka 2012, 2014; Boisvert et al. 2013; Wilhelm et al. 2015; Diogo et al. 2016; Miyake et al. 2016; Molnar et al. 2016; Regnault et al. 2017; and references therein) to establish, and use, the most common anatomical configuration for each taxon. In this survey, we found minimal or no clear discrepancies between studies; none of which would appreciably alter our results. Finally, because we focused on the muscular anatomy, we decided not to include any extinct taxa—for which there are only incomplete muscular reconstructions—in the present study. Our open dataset would allow future studies to add more extant and/or extinct taxa to modified analyses.

MODELING ANATOMICAL NETWORKS

We built skeletal and muscular network models of the pectoral and pelvic appendages of each species using the anatomical information gathered from dissections and the literature. A network model comprises a set of nodes and a set of links connecting the nodes (as in Fig. 2). Skeletal networks were modeled as undirected, unweighted networks in which nodes represent skeletal elements (ossified and cartilaginous) and links represent the presence of a physical joint or articulation between a pair of elements. Muscular networks were modeled as undirected, weighted networks in which nodes represent differentiated muscles and links represent the number of shared sites of anchoring (e.g., origin, insertion) between two muscles. Nodes disconnected from the largest

component of each network were excluded from these analyses because some functions did not tolerate disconnected nodes or yield unreliable values when they were present. The weights of links in muscular networks were ignored for the quantification of parameters for the same reasons, but they were considered for the search of connectivity modules.

ANATOMICAL NETWORK ANALYSIS

We measured seven network parameters to evaluate the anatomical organization of pectoral and pelvic appendages, namely: the total number of nodes (*N*) and of links (*K*), density of connections (*D*), mean clustering coefficient (*C*), mean shortest path length (*L*), heterogeneity of connections (*H*), and parcellation (*P*). Parameters *N*, *K*, *D*, *C*, *L*, and *H* were computed in R using algorithms implemented in the package *igraph* version 1.0.1 (Csardi and Nepusz 2006). Parameters *N* and *K* are simple counts of the number of elements and interactions modeled. Parameters *D*, *C*, *L*, and *H* are well-known parameters in network sciences; details on their mathematical equations were given elsewhere (Rasskin-Gutman and Esteve-Altava 2014). In short, *D* measures the actual number of connections divided by the maximum number possible (it ranges from 0 to 1). *C* measures the average of the ratio of a node's neighbors that connect among them (it ranges from 0 to 1). *L* measures the average number of links required to travel between two nodes (minimum 1). *H* measures the variability in the number of connections of nodes (minimum 0) as the ratio between the standard deviation and the mean of the number of connections of all nodes in the network. Finally, the parameter *P* was computed from the connectivity modules identified in the best partition of the network (see below); connectivity module are groups of nodes with more links to nodes within the group than to nodes outside the group. *P* is defined as $P = 1 - \sum_{m=1} (\frac{N_m}{N})^2$, where N_m is the number of nodes in module *m*, and *N* is the total number of nodes of the network. *P* is 0 when all nodes are in a same module, and *P* tends toward 1 when nodes are evenly distributed within many modules. To calculate *P*, we first needed to identify the number of modules and the nodes included in them. Connectivity modules were identified using the spin-glass model and simulated annealing algorithm (Reichardt and Bornholdt 2006) implemented in the package *igraph* for R. To account for stochasticity, we performed 1000 iterations of the algorithm and selected the best result. We provided the details of the modularity results in Tables S17–S29 for skeletal networks and Tables S39–S51 for muscular networks for further record.

The robustness of parameter values due to potential errors in identifying the particular bones and muscles and their connections from dissections was accounted by comparing the observed values to a randomly generated sample of 10,000 noisy networks for each one of the anatomical network of the study. A noisy network is generated by rewiring the links of the original musculoskeletal network with a probability of 5%; this introduces a 5% artificially generated error. To assess for robustness we compared observed values to the empirical distribution of values in the sample of noisy networks. Specifically, we tested the H_0 that observed value is equal to the sample mean. We rejected the H_0 with a *P*-value of 0.05 if the observed value is in the 5% end of the distribution of simulated values. Tables S7–S11 for skeletal networks and Tables S30–S34 for muscular networks summarize the sample mean, standard deviation, standard error of the mean, the interval for the 95% of simulated values, and the result of the empirical statistical test ("TRUE," we cannot reject H_0; "FALSE," we reject H_0 with *P*-value 0.05). A value of "TRUE" in Tables S11 and S34 means that the observed value of this parameter in this anatomical network is not different from the average measured in the sample of 10,000 noisy networks with artificially generated errors. This is the case for every parameter on every network, with a few exceptions, namely: parameter *H* in *Neoceratodus* pectoral and pelvic skeletal networks, parameter *C* in *Neoceratodus* pelvic muscular network, and parameter *P* in *Salamandra* and *Sphenodon* pelvic muscular networks. There is no way to generate random variation without creating unrealistic connections, that is, connections in which we could not in reality had made a dissection/coding error or for which no such natural variation exists (e.g., an ulnare connecting with a femur, or a pelvis disconnected from a femur). Unfortunately, manually curating the 10,000 noisy networks one by one is unfeasible in practice, whereas dissecting more specimens is not possible because they are endangered species and/or difficult to obtain and time-consuming to code for detailed network parameters.

QUANTIFICATION OF ANATOMICAL SIMILARITIES

We measured the similarity among appendages, and between pectoral and pelvic appendages, as the relative difference of values for each parameter, $d_r = (x - y)/((x + y)/2)$, where x and y are the two values compared. Results are shown as percentage of d_r for each pair of networks compared, and for each parameter, separately. We also computed the mean and standard deviation of d_r for the seven parameters in every comparison. Note that similarity is inversely related to d_r: higher values of d_r indicate lower similarity between appendages; likewise, lower values of d_r indicate greater similarity. Tables S1–S6 show the measured values.

PHYLOGENETIC COMPARISONS

With the sole purpose of helping to visualize the relative similarity among appendages, we plotted phylomorphospaces for every network parameter measured in skeletal and muscular networks. These plots project the phylogeny into a morphospace of two traits—values of a parameter for the pectoral and pelvic appendage—which allows us to compare visually the differences in similarity among taxa. Values for the pectoral appendages were

plotted along the *x*-axis; values for the pelvic appendage were plotted along the *y*-axis. For reference we added lines of equality, or identity, to phylomorphospaces to mark complete pectoral-pelvic similarity (*dashed red lines*), not to be confused with correlation lines. We created these phylomorphospaces using the function *phylomorphospace* in the R package *phytools* (Revell 2012). This function internally estimates the values for hypothetical taxonomic units using maximum likelihood. However, such estimations must be taken with caution because of the small sample size. For reference, we provided the reconstructed values and 95% CI in Tables S12 and S13 for skeletal networks and Tables S35 and S36 for muscular networks.

Limitations of our sample size, described above, prevent performing meaningful statistical tests. Nevertheless, for completeness, we have included in the Supporting Information the results of a Moran's I test of autocorrelation using neighboring weights (Tables S15 and S37). Moran's I tests were performed using the function *Moran.I* of the package *ape* (Paradis et al. 2004). Likewise, we performed correlations through the origin of phylogenetic independent contrasts between pectoral and pelvic appendages (Tables S16–S38). This test was performed using the functions *pic* and *lmorigin* of the package *ape*. As expected, parameters in pectoral and pelvic skeletal networks show nonsignificant phylogenetic autocorrelation; while only two parameters in pectoral muscular networks (*D*, *L*) and three (*D*, *L*, *H*) in pelvic muscular networks show a significant phylogenetic autocorrelation below the 5% significance level (and none of them below the 1%). In turn, pectoral and pelvic appendages correlate significatively for parameters of skeletal networks (which do not show phylogenetic autocorrelation), while only two out of seven correlations between pectoral and pectoral appendages in muscular networks are significant ($D_{\text{pec-pel}}$, $L_{\text{pec-pel}}$). Because of the small size of our sample, we have refrained from discussing these results further in the main text. This problem would not easily be ameliorated by including more extant tetrapods because more extant nontetrapods would then need inclusion to prevent imbalance in the analyses.

Phylogenetic visualizations and tests were performed using a consensus phylogeny of the studied taxa created using information from Tree of Life Web Project (Janvier 1997). Branch lengths were calibrated in millions of years of evolution for the minimal divergence time of each taxa crown group according to the Paleobiological Database (available at https://paleobiodb.org/). For example, the split of *Sphenodon* from the two salamanders was set as the split between amniotes (Reptiliomorpha) and lissamphibians (Temnospondyli), 312 Ma. Note that the branch lengths shown in phylomorphospaces do not correspond to the actual tree lengths, but represent differences in the values of parameters among taxa.

AUTHORS CONTRIBUTION

B.E.-A. designed the study.

B.E.-A., J.L.M., and R.D. collected network data from *Polypterus* and *Ambystoma* specimens. P.J. collected network data from *Neoceratodus* and *Latimeria* specimens.

J.R.H. collected network data from *Salamandra* and *Sphenodon* specimens. B.E.-A. scripted and performed the networks analyses.

B.E.-A. and J.L.M. prepared the figures. B.E.-A. wrote the manuscript. All authors discussed the results and revised the manuscript.

ACKNOWLEDGMENTS

We thank Jean Joss (Macquarie Univ.) for providing dipnoan specimens, Wolfgang Maier, Erich Weber (Universität Tübingen), the California Academy of Sciences (USA), and the Natural History Museum (UK) for allowing dissection of their material. Lawrence Frank and Rachel Berquist (UCSD; NSF Grant DBI-0446389) for the MRI scans. Liam Revell and Sandy Kawano for their advice on comparative methods. Marta Sales-Pardo for her advice in testing network parameters robustness. Matt Friedman, Hans Larson, and three anonymous reviewers for their feedback during the review processes. We also appreciate the input of Krijn Michel, Stephanie Pierce, and Sophie Regnault.

This project is funded by the European Union's Horizon 2020 research and innovation program under the Marie Skłodowska-Curie grant agreement No 654155.

CONFLICT OF INTEREST

The authors declare no conflicts of interest.

LITERATURE CITED

Abbasi, A. A. 2011. Evolution of vertebrate appendicular structures: insight from genetic and palaeontological data. Dev. Dyn. 240:1005–1016.

Ahlberg, P. E. 1989. Paired fin skeletons and relationships of the fossil group Porolepiformes (Osteichthyes: Sarcopterygii). Zool. J. Linn. Soc. 96:119–166.

———. 2011. Humeral homology and the origin of the tetrapod elbow: a reinterpretation of the enigmatic specimens ANSP 21350 and GSM 104536. Spec. Pap. Palaeontol. 86:17–29.

Andrews, S. M., and T. S. Westoll. 1970. The postcranial skeleton of *Eusthenopteron foordi* Whiteaves. Earth Environ. Sci. Trans. R Soc. Edinb. 68:207–329.

Boisvert, C. A. 2005. The pelvic fin and girdle of *Panderichthys* and the origin of tetrapod locomotion. Nature 438:1145–1147.

Boisvert, C. A., J. M. Joss, and P. E. Ahlberg. 2013. Comparative pelvic development of the axolotl (*Ambystoma mexicanum*) and the Australian lungfish (*Neoceratodus forsteri*): conservation and innovation across the fish-tetrapod transition. Evodevo 4:3.

Boisvert, C. A., E. Mark-Kurik, and P. E. Ahlberg. 2008. The pectoral fin of *Panderichthys* and the origin of digits. Nature 456:636–638.

Coates, M. I., and J. A. Clack. 1990. Polydactyly in the earliest known tetrapod limbs. Nature 347:66–69.

Coates, M. I., and M. J. Cohn. 1998. Fins, limbs, and tails: outgrowths and axial patterning in vertebrate evolution. BioEssays 20:371–381.

———. 1999. Vertebrate axial and appendicular patterning: the early development of paired appendages. Am. Zool. 39:676–685.

Coates, M. I., J. E. Jeffery, and M. Ruta. 2002. Fins to limbs: what the fossils say. Evol. Dev. 4:390–401.

Csardi, G., and T. Nepusz. 2006. The igraph software package for complex network research. InterJ. Complex Syst. 1659:1–9.

Diogo, R., and V. Abdala. 2010. Muscles of vertebrates–comparative anatomy, evolution, homologies and development. Science Publishers, Enfield.

Diogo, R., B. Esteve-Altava, C. Smith, J. C. Boughner, and D. Rasskin-Gutman. 2015. Anatomical network comparison of human upper and lower, newborn and adult, and normal and abnormal limbs, with notes on development, pathology and limb serial homology vs. homoplasy. PLoS ONE 10:e0140030.

Diogo, R., P. Johnston, J. L. Molnar, and B. Esteve-Altava. 2016. Characteristic tetrapod musculoskeletal limb phenotype emerged more than 400 MYA in basal lobe-finned fishes. Sci. Rep. 6:37592.

Diogo, R., M. Linde-Medina, V. Abdala, and M. A. Ashley-Ross. 2013. New, puzzling insights from comparative myological studies on the old and unsolved forelimb/hindlimb enigma. Biol. Rev. 88:196–214.

Diogo, R., and J. Molnar. 2014. Comparative anatomy, evolution, and homologies of tetrapod hindlimb muscles, comparison with forelimb muscles, and deconstruction of the forelimb-hindlimb serial homology hypothesis. Anat. Rec. 297:1047–1075.

Diogo, R., and E. M. Tanaka. 2012. Anatomy of the pectoral and forelimb muscles of wild-type and green fluorescent protein-transgenic axolotls and comparison with other tetrapods including humans: a basis for regenerative, evolutionary and developmental studies. J. Anat. 221: 622–635.

———. 2014. Development of fore- and hindlimb muscles in GFP-transgenic axolotls: morphogenesis, the tetrapod bauplan, and new insights on the forelimb-hindlimb enigma. J. Exp. Zool. B Mol. Dev. Evol. 322:106–127.

Diogo, R., and J. M. Ziermann. 2015. Muscles of chondrichthyan paired appendages: comparison with Osteichthyans, deconstruction of the fore–hindlimb serial homology dogma, and new insights on the evolution of the vertebrate neck. Anat. Rec. 298:513–530.

Eble, G. J. 2005. Morphological modularity and macroevolution. Pp. 221–238 *in* W. Callebaut and D. Rasskin-Gutman, eds. Modularity: Understanding the development and evolution of natural complex systems. The MIT Press, Cambridge.

Esteve-Altava, B. 2017a. Challenges in identifying and interpreting organizational modules in morphology. J. Morphol. 278:960–974.

———. 2017b. In search of morphological modules: a systematic review. Biol. Rev. 92:1332–1347.

Esteve-Altava, B., J. Marugán-Lobón, H. Botella, and D. Rasskin-Gutman. 2011. Network models in anatomical systems. J. Anthropol. Sci. 89:175–184.

Francis, E. T. B. 1934. The anatomy of the salamander. The Clarendon Press, Oxford.

Goodrich, E. S. 1930. Studies on the structure and development of vertebrates. Macmillan, London.

Goswami, A., W. J. Binder, J. Meachen, and F. R. O'Keefe. 2015. The fossil record of phenotypic integration and modularity: a deep-time perspective on developmental and evolutionary dynamics. Proc. Natl. Acad. Sci. 112:4891–4896.

Goswami, A., J. B. Smaers, C. Soligo, and P. D. Polly. 2014. The macroevolutionary consequences of phenotypic integration: from development to deep time. Philos. Trans. R Soc. B Biol. Sci. 369:20130254.

Hallgrímsson, B., K. Willmore, and B. K. Hall. 2002. Canalization, developmental stability, and morphological integration in primate limbs. Am. J. Phys. Anthropol. 119:131–158.

Irisarri, I., D. Baurain, H. Brinkmann, F. Delsuc, J. Y. Sire, A. Kupfer, J. Petersen, M. Jarek, A. Meyer, M. Vences, et al. 2017. Phylotranscriptomic consolidation of the jawed vertebrate timetree. Nat. Ecol. Evol. 1: 1370.

Janvier, P. 1997. Vertebrata. Animals with backbones. The tree of life web project. Available at http://tolweb.org/Vertebrata/14829/1997.01.01.

Jardine, N. 1969. A logical basis for biological classification. Syst. Zool. 18:37.

Johanson, Z., J. Joss, C. A. Boisvert, R. Ericsson, M. Sutija, and P. E. Ahlberg. 2007. Fish fingers: digit homologues in sarcopterygian fish fins. J. Exp. Zool. B Mol. Dev. Evol. 308:757–768.

Kerkman J. N., A. Daffertshofer, L. Gollo, M. Breakspear, T. W. Boonstra. 2017. Network structure of the human musculoskeletal system shapes neural interactions on multiple timescales. bioRxiv 181818; https://doi.org/10.1101/181818.

Klingenberg, C. P. 2008. Morphological integration and developmental modularity. Annu. Rev. Ecol. Evol. Syst. 39:115–132.

Kolarov, N. T., A. Ivanović, and M. L. Kalezić. 2011. Morphological integration and ontogenetic niche shift: a study of crested newt limbs. J. Exp. Zool. B Mol. Dev. Evol. 316:296–305.

Larouche, O., R. Cloutier, and M. L. Zelditch. 2015. Head, body and fins: patterns of morphological integration and modularity in fishes. Evol. Biol. 42:296–311.

Larouche, O., M. L. Zelditch, and R. Cloutier. 2017. Fin modules: an evolutionary perspective on appendage disparity in basal vertebrates. BMC Biol. 15:32.

Martín-Serra, A., B. Figueirido, J. A. Pérez-Claros, and P. Palmqvist. 2015. Patterns of morphological integration in the appendicular skeleton of mammalian carnivores. Evolution 69:321–340.

Maxwell, E. E., and T. A. Dececchi. 2012. Ontogenetic and stratigraphic influence on observed phenotypic integration in the limb skeleton of a fossil tetrapod. Paleobiology 39:123–134.

Millot, J., and J. Anthony. 1958. Anatomie de Latimeria chalumnae. Tome I. Squelette, muscles, et formation de soutiens. Centre National de la Recherche Scientifique, Paris.

Miyake, T., M. Kumamoto, M. Iwata, R. Sato, M. Okabe, H. Koie, N. Kumai, K. Fujii, K. Matsuzaki, C. Nakamura, et al. 2016. The pectoral fin muscles of the coelacanth *Latimeria chalumnae*: functional and evolutionary implications for the fin-to-limb transition and subsequent evolution of tetrapods. Anat. Rec. 299:1203–1223.

Miyashita, T., and R. Diogo. 2016. Evolution of serial patterns in the vertebrate pharyngeal apparatus and paired appendages via assimilation of dissimilar units. Front. Ecol. Evol. 4:71.

Molnar, J. L., P. S. Johnston, B. Esteve-Altava, and R. Diogo. 2016. Musculoskeletal anatomy of the pelvic fin of *Polypterus*: implications for phylogenetic distribution and homology of pre- and postaxial pelvic appendicular muscles. J. Anat. 230:532–541.

Molnar, J. L., R. Diogo, J. R. Hutchinson, and S. E. Pierce. 2017. Reconstructing pectoral appendicular muscle anatomy in fossil fish and tetrapods over the fins-to-limbs transition. Biol. Rev. published online. https://doi.org/10.1111/brv.12386.

Murphy, A. C., S. F. Muldoon, D. Baker, A. Lastowka, B. Bennett, M. Yang, and D. S. Bassett. 2018. Structure, function, and control of the musculoskeletal network. PLoS Biol. 16:e2002811.

Nakamura, T., A. R. Gehrke, J. Lemberg, J. Szymaszek, and N. H. Shubin. 2016. Digits and fin rays share common developmental histories. Nature 537:225–228.

Owen, R. 1849. On the nature of limbs: A discourse. J van Voorst, London.

Paradis, E., J. Claude, and K. Strimmer. 2004. APE: analyses of phylogenetics and evolution in R language. Bioinformatics 20:289–290.

Rasskin-Gutman, D., and B. Esteve-Altava. 2014. Connecting the dots: anatomical network analysis in morphological. EvoDevo. Biol. Theory 9:178–193.

Regnault, S., J. R. Hutchinson, and M. E. H. Jones. 2017. Sesamoid bones in tuatara (*Sphenodon punctatus*) investigated with X-ray microtomography, and implications for sesamoid evolution in Lepidosauria. J. Morphol. 278:62–72.

Reichardt, J., and S. Bornholdt. 2006. Statistical mechanics of community detection. Phys. Rev. E Stat. Nonlin. Soft Matter. Phys. 74(1 Pt 2):016110 https://www.ncbi.nlm.nih.gov/pubmed/16907154.

Remane, A. 1956. Die Grundlagen des natürlichen Systems, der vergleichenden Anatomie und der Phylogenetik. Geest und Portig, Leipzig.

Revell, L. J. 2012. phytools: an R package for phylogenetic comparative biology (and other things). Methods Ecol. Evol. 3:217–223.

Ruvinsky, I., and J. J. Gibson-Brown. 2000. Genetic and developmental bases of serial homology in vertebrate limb evolution. Development 127:5233–5244.

Santos, D. A. D., J. Fratani, M. L. Ponssa, and V. Abdala. 2017. Network architecture associated with the highly specialized hindlimb of frogs. PLOS ONE 12:e0177819.

Sears, K. E., T. D. Capellini, and R. Diogo. 2015. On the serial homology of the pectoral and pelvic girdles of tetrapods. Evolution 69:2543–2555.

Shubin, N. H., E. B. Daeschler, and F. A. Jenkins. 2006. The pectoral fin of *Tiktaalik roseae* and the origin of the tetrapod limb. Nature 440:764–771.

———. 2014. Pelvic girdle and fin of *Tiktaalik roseae*. Proc. Natl. Acad. Sci. 111:893–899.

Shubin, N., C. Tabin, and S. Carroll. 1997. Fossils, genes and the evolution of animal limbs. Nature 388:639–648.

Simon, H. A. 1962. The architecture of complexity. Proc. Am. Philos. Soc. 106:467–482.

Sordino, P., F. van der Hoeven, D. Duboule. 1995. Hox gene expression in teleost fins and the origin of vertebrate digits. Nature 375:678–681.

Villmoare, B., J. Fish, and W. Jungers. 2011. Selection, morphological integration, and strepsirrhine locomotor adaptations. Evol. Biol. 38:88–99.

Wagner, G. P. 1989. The biological homology concept. Annu. Rev. Ecol. Syst. 20:51–69.

———. 2014. Homology, genes, and evolutionary innovations. Princeton Univ. Press, Princeton.

Wagner, G. P., M. Pavlicev, and J. M. Cheverud. 2007. The road to modularity. Nat. Rev. Genet. 8:921–931.

Weiss, P. A. 1971. The basic concept of hierarchic systems. Pp. 1–44 *in* P. A. Weiss, ed. Hierarchically organized systems in theory and practice. Hafner Publishing Company, New York.

Wilhelm, B. C., T. Y. Du, E. M. Standen, and H. C. Larsson. 2015. *Polypterus* and the evolution of fish pectoral musculature. J. Anat. 226:511–22.

Wilson, M. V., G. F. Hanke, and T. Märss. 2007. Paired fins of jawless vertebrates and their homologies across the "agnathan"-gnathostome transition. Pp. 122–149 *in* J. S. Anderson and H.-D. Sues, eds. Major transitions in vertebrate evolution. Indiana Univ. Press, Bloomington.

Witmer, L. M. 1995. The extant phylogenetic bracket and the importance of reconstructing soft tissues in fossils. Pp. 17–33 *in* J. Thomason, ed. Functional morphology in vertebrate paleontology. Cambridge Univ. Press, Cambridge, UK.

Woltering, J. M., and D. Duboule. 2010. The origin of digits: expression patterns versus regulatory mechanisms. Dev. Cell 18:526–532.

Yano, T., and K. Tamura. 2013. The making of differences between fins and limbs. J. Anat. 222:100–113.

Young, G. C., R. E. Barwick, and K. S. W. Campbell. 1989. Pelvic girdles of lungfishes (Dipnoi). Pp. 59–75 *in* R. W. LeMaitre, ed. Pathways in geology: Essays in honour of Edwin Sherbon Hills. Blackwell Scientific, Melbourne.

Young, N. M., B. Hallgrímsson, and C. Janis. 2005. Serial homology and the evolution of mammalian limb covariation structure. Evolution 59:2691–2704.

Young, N. M., G. P. Wagner, and B. Hallgrímsson. 2010. Development and the evolvability of human limbs. Proc. Natl. Acad. Sci. 107:3400–3405.

Associate Editor: M. Friedman
Handling Editor: M. Servedio

Supporting Information

Additional Supporting Information may be found in the online version of this article at the publisher's website:

Figure S1. Relative differences between pectoral and pelvic skeleton.
Figure S2. Relative differences between pectoral and pelvic musculature.
Table S1. Percentage of relative difference of parameters among pectoral skeletal networks.
Table S2. Percentage of relative differences of parameters among pelvic skeletal networks.
Table S3. Percentage of relative difference between pectoral and pelvic skeletal networks.
Table S4. Percentage of relative difference of parameters among pectoral muscular networks.
Table S5. Percentage of relative differences of parameters among pelvic muscular networks.
Table S6. Percentage of relative difference between pectoral and pelvic muscular networks.
Table S7. Mean values of parameters in 10000 noisy skeletal networks.
Table S8. SD values of parameters in 10000 noisy skeletal networks.
Table S9. SEM values of parameters in 10000 noisy skeletal networks.
Table S10. Inter 95% distribution range values of parameters in 10000 noisy skeletal networks.
Table S11. Test of observed values in skeletal network falling within the 95% range of 10000 noisy skeletal networks.
Table S12. Ancestral state reconstruction of pectoral skeletal network parameters (95% CIs).
Table S13. Ancestral state reconstruction of pelvic skeletal network parameters (95% CIs).
Table S14. Moran's I test of autocorrelation on skeletal networks parameters.
Table S15. Regression through the origin of phylogenetic independent contrasts for pectoral-pelvic skeletal networks.
Table S16. Summary of the modularity analysis in skeletal networks.
Table S17. Connectivity modules in the pectoral skeletal network of *Polypterus*.
Table S18. Connectivity modules in the pelvic skeletal network of *Polypterus*.
Table S19. Connectivity modules in the pectoral skeletal network of *Latimeria*.
Table S20. Connectivity modules in the pelvic skeletal network of *Latimeria*.
Table S21. Connectivity modules in the pectoral skeletal network of *Neoceratodus*.
Table S22. Connectivity modules in the pelvic skeletal network of *Neoceratodus*.
Table S23. Connectivity modules in the pectoral skeletal network of *Ambystoma*.
Table S24. Connectivity modules in the pelvic skeletal network of *Ambystoma*.
Table S25. Connectivity modules in the pectoral skeletal network of *Salamandra*.
Table S26. Connectivity modules in the pelvic skeletal network of *Salamandra*.
Table S27. Connectivity modules in the pectoral skeletal network of *Sphenodon*.
Table S28. Connectivity modules in the pelvic skeletal network of *Sphenodon*.
Table S29. Mean values of parameters in 10000 noisy muscular networks.
Table S30. SD values of parameters in 10000 noisy muscular networks.
Table S31. SEM values of parameters in 10000 noisy muscular networks.
Table S32. Inter 95% distribution range values of parameters in 10000 noisy muscular networks.
Table S33. Test of observed values in muscular network falling within the 95% range of 10000 noisy muscular networks.
Table S34. Ancestral state reconstruction of pectoral muscular network parameters (95% CIs).
Table S35. Ancestral state reconstruction of pelvic muscular network parameters (95% CIs).
Table S36. Moran's I test of autocorrelation on muscular networks parameters.
Table S37. Regression through the origin of phylogenetic independent contrasts for pectoral-pelvic muscular networks.
Table S38. Summary of the modularity analysis in muscular networks.
Table S39. Connectivity modules in the pectoral muscular network of *Polypterus*.
Table S40. Connectivity modules in the pelvic muscular network of *Polypterus*.
Table S41. Connectivity modules in the pectoral muscular network of *Latimeria*.
Table S42. Connectivity modules in the pelvic muscular network of *Latimeria*.
Table S43. Connectivity modules in the pectoral muscular network of *Neoceratodus*.
Table S44. Connectivity modules in the pelvic muscular network of *Neoceratodus*.
Table S45. Connectivity modules in the pectoral muscular network of *Ambystoma*.
Table S46. Connectivity modules in the pelvic muscular network of *Ambystoma*.
Table S47. Connectivity modules in the pectoral muscular network of *Salamandra*.
Table S48. Connectivity modules in the pelvic muscular network of *Salamandra*.
Table S49. Connectivity modules in the pectoral muscular network of *Sphenodon*.
Table S50. Connectivity modules in the pelvic muscular network of *Sphenodon*.